

Nucleation scenarios for wetting transition on textured surfaces: The effect of contact angle hysteresis

C. ISHINO and K. OKUMURA(*)

*Department of Physics, Graduate School of Humanities and Sciences
Ochanomizu University - 2-1-1, Otsuka, Bunkyo-ku, Tokyo 112-8610, Japan*

received 3 July 2006; accepted in final form 11 September 2006

published online 7 October 2006

PACS. 68.08.Bc – Wetting.

PACS. 05.70.Np – Interface and surface thermodynamics.

PACS. 81.65.-b – Surface treatments.

Abstract. – The wettability of textured surfaces is strongly dependent on the contact state of a small drop deposited on them. We consider transitions via nucleation between two representative contact states of Cassie and Wenzel when there exists hysteresis in the contact angle. We find that the effect of the hysteresis is significant: a drop can be trapped by various states which are neither Cassie nor Wenzel states in the conventional sense.

Introduction. – Recently, wetting properties of surfaces artificially textured at submicron or nano scales have attracted a considerable attention; the possibility to tune textures to attain desired purposes has been actively explored by experiments, simulations, and theories [1–16]. On such textured surfaces, the contact state of a liquid drop controls the wetting property. Possible contact states include the Cassie state (fig. 3a below) where air is trapped between the bottom of the liquid drop and the solid surface and the Wenzel state (fig. 3c below) where liquid at the contact may penetrate into the texture; the latter Wenzel drop is very sticky, showing high contact angle hysteresis, while the former Cassie drop easily rolls on the surface by small perturbation. The transition between them is discussed in this paper.

We consider a model surface textured by a forest of cylindrical pillars arranged in a square lattice with a lattice constant L , where the radius and height of the pillars are b and h , respectively, as in fig. 1. The surface roughness r is given as the ratio of the actual area to the projected area: $r = 1 + 2\pi bh/L^2$. The solid fraction ϕ of the contact circle at the bottom of the Cassie drop can be represented by $\phi = \pi b^2/L^2$.

On the textured surface, we deposit a spherical liquid drop of radius R_0 small enough to neglect gravity. At equilibrium, the shape of the drop is characterized by the radius of the contact circle given by $X \equiv R \sin \theta$ together with the contact angle θ as in fig. 2. Here, the radius R is determined by equating the volume of the drop in fig. 2 with the original volume, $4\pi R_0^3/3$ (the volume of liquid penetrated into textures is always negligible: $R_0 \gg b, h, L$):

$$R/R_0 = 4^{1/3}(2 - 3 \cos \theta + \cos^3 \theta)^{-1/3}. \quad (1)$$

The contact angle θ is determined to minimize the surface energy for a given contact state. As a result, the contact angles of the Wenzel drop and of the Cassie drop are given

(*) E-mail: okumura@phys.ocha.ac.jp (corresponding author)

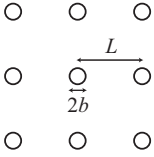


Fig. 1

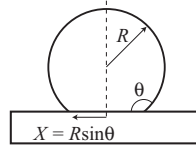


Fig. 2

Fig. 1 – Top view of the surface textured by pillars.

Fig. 2 – A drop placed on a surface. The liquid-air interface of the drop shall be called a spherical cap, whose area is S_C . The area of the bottom planer contact circle of radius $R \sin \theta$ shall be denoted S_B .

by $\cos \theta_W = r \cos \theta_0$ and $\cos \theta_C = \phi \cos \theta_0 - (1 - \phi)$, respectively, where the contact angle of the original flat surface is θ_0 [17]. The corresponding R takes a value $R_W \equiv R(\theta_W)$ for the Wenzel state and $R_C \equiv R(\theta_C)$ for the Cassie state, with $R(\theta)$ defined in eq. (1).

The surface energy E_1 of a drop placed on a textured surface with the contact angle θ is simplified when $\theta = \theta_W$ or θ_C [18]:

$$E_1/E_0 = 2^{-2/3} (2 - 3 \cos \theta + \cos^3 \theta)^{1/3} \tag{2}$$

which is an increasing function of θ . Here, $E_0 \equiv 4\pi R_0^2 \gamma$ is the surface energy of the original spherical drop where γ is the surface energy of the liquid.

When $\theta_W < \theta_C$, the Wenzel drop surface energy is lower than the Cassie drop energy because E_1 in eq. (2) is an increasing function of θ : in terms of energy the Wenzel state is expected. In experiments, however, even when $\theta_W < \theta_C$, the drop could be in the Cassie state at first and then changed into the Wenzel state by small perturbation: the Cassie state could be a metastable state separated from the stable Wenzel state by an energy barrier. This barrier problem was studied by two groups [9, 18] in the same spirit, without taking into account the contact angle hysteresis (CAH). In this study, we examine the barrier under the influence of CAH in a different mode of transition. We note that the effect of CAH is recently considered also in ref. [19] in a different context of impact of drops.

Nucleation of Wenzel contact. – For the barrier estimation, we assume that the transition from the Cassie to Wenzel state starts from the center (see fig. 3): a nucleus of a *Wenzel contact* is formed at the center for some reason and then it begins to grow. Here, the Wenzel contact is a region inside which liquid is penetrated into the grooves as in the Wenzel state and outside which air is trapped as in the Cassie state. We expect this nucleation scenario when there exists a certain inhomogeneity around the center (possibly due to a slight effect of gravity and/or to a defect of texture). We consider below the case where $\theta_W < \theta_C$, because this situation has been often discussed in the literature.

Once nucleation growth starts, the radius x of the Wenzel contact gets larger while the radius X of the apparent contact circle could move independently (of x) in general (we consider below only the region $X \geq x$; the surface energy always increases as x exceeds X , because of the creation of an extra liquid-air surface in addition to liquid-solid surface): *intermediate states can be specified by the parameters x and X* (fig. 3b).

Surface energy of intermediate states. – We can calculate the surface energy $E_s(x, X)$ of the state specified by (x, X) . The result can be cast into the following form:

$$E_s(x, X)/\gamma = S_C(X) - \cos \Theta(x, X) S_B(X), \tag{3}$$

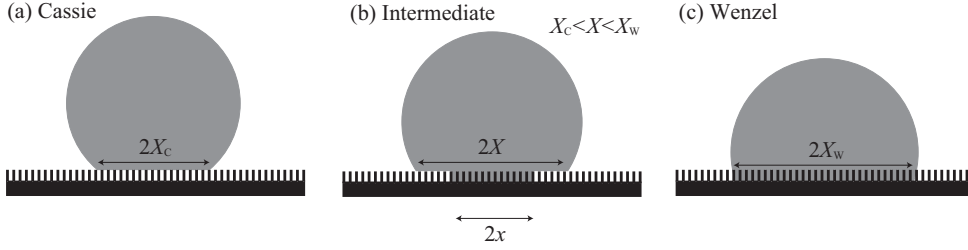


Fig. 3 – Cassie-Wenzel transition by nucleation. Air is trapped at the contact in the Cassie state (a), while liquid penetrates into the texture in the Wenzel state (c). The transition between the two states progresses with the growth of a circular region (Wenzel contact) of radius x at the bottom (b). The radius of apparent contact circle X ($> x$) may change during this process.

where $S_C(X)$ and $S_B(X)$ are the area of the spherical cap and of the bottom circle for a given X (see fig. 2). Note that the radius R and the angle θ in fig. 2 can be determined from the condition of volume conservation of the drop for a given X , and thus $S_C(X)$ and $S_B(X)$ can be calculated for a given X via numerical root finding. The parameter $\Theta(x, X)$ is given as

$$\cos \Theta(x, X) = f_W \cos \theta_W + (1 - f_W) \cos \theta_C, \quad (4)$$

where $f_W = x^2/X^2$ is the area fraction of the nucleus at the contact (fig. 3b). Note that the parameter $\Theta(x, X)$ is in general different from the angle θ in fig. 2 (the latter angle is determined by geometry while the former by area fractions of the Wenzel and Cassie contacts under the drop); otherwise eq. (3) would be reduced to a simpler form given in eq. (2).

The energy $E \equiv E_s(x, X)$ numerically obtained is plotted in fig. 4 for typical parameters (specified in the first line of table I). On the left plot, the point on the surface $P_C = (x = 0, X = X_C, E = E_C)$ represents the Cassie state where $X_C \equiv R_C \sin \theta_C (= 0.302R_0)$ and $E_C = E_s(0, X_C)$ because this state is specified by $(x, X) = (0, X_C)$. Likewise, the point $P_W = (X_W, X_W, E_W)$ on the surface represents the Wenzel state where $X_W \equiv R_W \sin \theta_W (= 0.914R_0)$ and $E_W = E_s(X_W, X_W)$. When a drop is initially in the Cassie state at P_C , it tends to follow the steepest descent path on the surface to minimize the energy down to the final Wenzel state at P^* .

We have checked that the steepest path here is the shortest line (*i.e.*, the straight line on the right contour plot) connecting P_C and $P_{CW} = (X_C, X_C, E')$, followed by the shortest line connecting P_{CW} and P_W (There is no energy barrier in this transition pathway once the initial nucleation patch is created, where the patch energy is about γL^2). This suggests the following fate of this drop: X (specifying the position of a *macroscopic circular contact line*) remains to be the initial Cassie value X_C until x (size of the nucleus) reaches X_C and, after this, $x (= X)$ grows to the final value X_W .

It would be difficult to see that the steepest descent path from P_C to P_{CW} is the shortest

TABLE I – Parameters used in numerical estimates. h, b, L are given in μm while the angles are in deg. The equilibrium contact angle is $\theta_0 = 110$ deg and the radius of the drop is $R_0 = 1$ mm in both cases.

h	b	L	r	ϕ	θ_W	θ_C	X_C/R_0	X_W/R_0
5	1.5	10	1.47	0.0707	120	163	0.302	0.914
10	1.5	10	1.94	0.0707	132	163	0.302	0.767

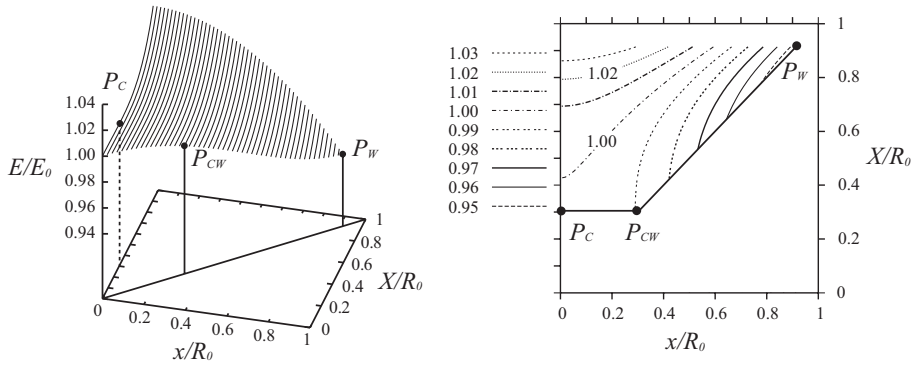


Fig. 4 – Energy landscape without CAH. The energy surface on the left is cut by the three planes defined by the equations $x = 0$, $X = X_W (= 0.914R_0)$, and $x = X$, respectively, to show the region of interest. The steepest descent paths from P_C to P_{CW} and from P_{CW} to P_W are the shortest lines connecting them, as indicated on the right contour plot of E/E_0 .

line between them on the scale of fig. 4, but there exists a steep valley along the line on the scale of thermal energy (see below). This would be reasonable since the Cassie state is the minimum of the variable X at $x = 0$.

The criterion for the nucleation growth can be discussed in terms of competition between the energy of the circular surface of the nucleus and that of the peripheral surface of the nucleus. The former is given by $-\pi x^2 \gamma (\cos \theta_W - \cos \theta_C)$ while the latter by $2\pi x h \gamma (1 - \phi)$. This leads to a critical size of the nucleus of the order of h in our parameter range. This indicates that the smallest initial patch ($x \simeq L$) is already above the critical size so that the peripheral energy could be neglected below.

Energy associated with CAH. – If CAH is nonzero, one has to apply a force $\gamma \delta^{(i)}$ (per unit length of the contact line) to move the contact line on pillar surfaces and on the bottom flat surface (the plane where pillars are built). Here, CAH is specified by $\delta^{(i)}$:

$$\delta^{(i)} = \cos \theta^{(i)} - \cos \theta_A^{(i)}. \tag{5}$$

Note that the equilibrium contact angle $\theta^{(i)}$ and the advancing angle $\theta_A^{(i)}$ on the pillar surface ($i = p$) or the bottom flat surface ($i = b$) might be different from those on the original flat surface (*e.g.*, the surface of pillar side is often very rough, as often shown in a microscopic photograph). We neglect below the CAH on the pillar top for simplicity, which is appropriate for $\phi \ll 1$.

The energy required to move the contact line of length $2\pi b$ around a pillar from the top down to the bottom by a distance h is given by $2\pi b h \gamma \delta^{(p)}$. This expression is actually independent of the direction of invasion (*e.g.*, when a pillar is invaded from the side the contact line of length h moves by a distance $2\pi b$, resulting in the same energy, $2\pi b h \gamma \delta^{(p)}$). The energy of friction with pillars for a nucleus of radius x is thus given by

$$E_p(x) = 2\pi b h \gamma \delta^{(p)} \cdot \pi x^2 / L^2. \tag{6}$$

Similarly, the energy of friction with the bottom flat surface is given by

$$E_b(x) = 2\pi x^2 (1 - \phi) \gamma \delta^{(b)}. \tag{7}$$

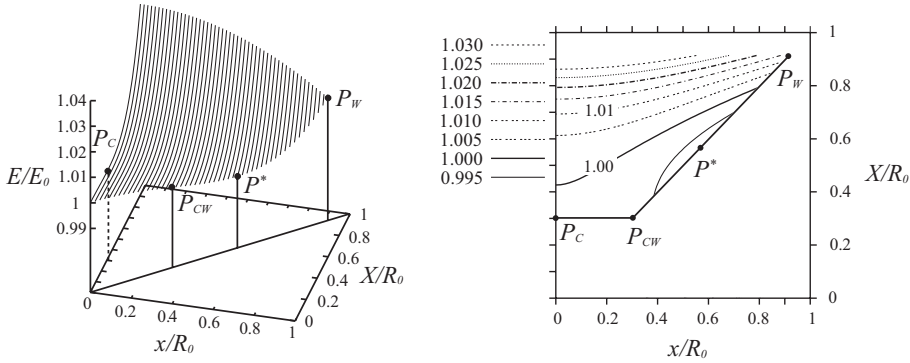


Fig. 5 – Energy landscape with a moderate CAH ($\Delta = 15$ deg). The steepest descent paths from P_C to P_{CW} and from P_{CW} to P^* are again the shortest lines connecting the adjacent points.

Fate of drops with CAH. – It is convenient to consider the total energy required to attain a state represented by (x, X) : $E(x, X) = E_s + E_p + E_b$. The required energy is uniquely determined by (x, X) for the process in which x keeps increasing, although $E(x, X)$ is not the potential energy (the friction force is not conservative): The energy landscape indicates the direction of change of our nucleation process on the (x, X) -plane. This E for a moderate CAH ($\Delta \equiv \theta_A^{(i)} - \theta^{(i)} = 15$ deg, independent of i), with the other parameters given in the first line in table I, is shown in fig. 5. Here, we find the following scenario: the drop starts from the point $P_C = (0, X_C, E_C)$ to $P_{CW} = (X_C, X_C, E')$ and down to $P^* = (X^*, X^*, E^*)$, following the steepest descent path, and may stay there: the drop at P^* has to climb an uphill to go to P_W (unlike the situation in fig. 4) because external energy is required to move the contact line. The trapped state represented by P^* is neither the Cassie nor the Wenzel state in the conventional sense: liquid is fully penetrated at the whole contact circle as in the Wenzel state but the contact angle θ^* is different from θ_W ($\theta_W < \theta^* < \theta_C$).

With a stronger CAH but still in a realistic range ($\Delta = 30$ deg), the drop starting from $P_C = (0, X_C, E_C)$ sees an uphill in any direction (fig. 6): the Cassie drop remains to be in the state without an energy input from the exterior, as may be typically observed in experiments. When the drop gets an energy from outside, it would seek the easiest uphill up to P_W on the surface of the left plot in fig. 6. When the applied energy is used up to go the uphill up to

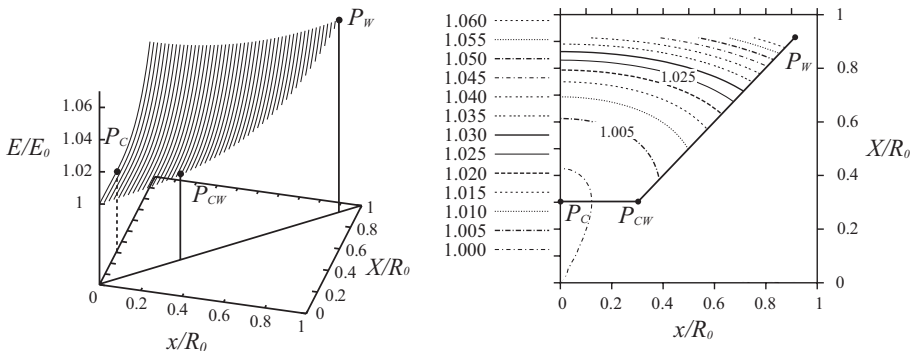


Fig. 6 – Energy landscape with a moderate CAH ($\Delta = 30$ deg).

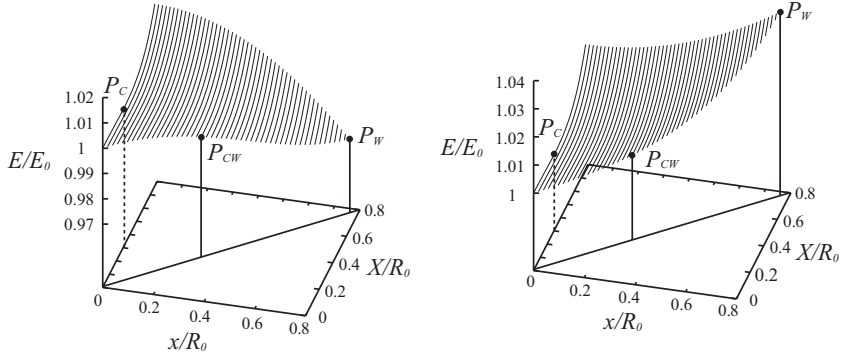


Fig. 7 – Energy landscape for $h = 10 \mu\text{m}$: (left) $\Delta = 0 \text{ deg}$ and (right) $\Delta = 15 \text{ deg}$.

somewhere between P_C and P_W , it cannot roll down the slope and stay there because such a movement is always accompanied by the movement of the contact line and thus requires an energy (here, E is not a potential energy).

When the pillar becomes higher (fig. 7; see the second line in table I for parameters), although there exists no barrier from the Cassie state to the Wenzel state (once nucleation starts) if CAH is absent, the effect of CAH (if it exists) is stronger (than in figs. 5 and 6). This is due to an increase in dissipation associated with higher pillar walls: the Cassie state tends to be meta-stabilized more easily.

We here comment on the roll of thermal fluctuations in this problem. The energy scale kT (the Boltzmann constant times temperature) is much smaller than a typical surface energy: $kT/E_0 \simeq (a/R_0)^2 \simeq 10^{-14}$, where a is a molecular scale. This implies the trapped state in the above is metastable for thermal fluctuations. In addition, the thermal energy is too small to create the initial nucleation patch, which requires an energy γL^2 ($L \simeq \mu\text{m}$): $kT/\gamma L^2 \simeq (L/R_0)^2 \simeq 10^{-9}$. This implies that, even without CAH, there is a barrier of the order of γL^2 between the Cassie and the Wenzel states, if there exist no defects in the texture.

Conclusion. – We have considered a nucleation of the Wenzel contact from the center of the Cassie state, as a representative case with inhomogeneity at the contact circle, in the regime where the Wenzel state has lower surface energy. The transition pathway from the Cassie to Wenzel state without CAH is clarified: the macroscopic circular contact line (specified X) is pinned till a nucleus size catches up with the size of the initial Cassie contact circle (specified X_C). With CAH, the landscape of the energy, which includes the hysteresis term, is helpful to understand the fate of a drop on a textured substrate: the macroscopic contact line (specified X) of a drop always prefers the pinning in the above sense during transitions by nucleation. We find that a drop could be trapped in a state which is neither Cassie nor Wenzel state, with a modest CAH. With a larger CAH, but still in the range of typical values, the drop can be trapped by various states depending on the energy applied to the drop as an external perturbation. Similar effects are also important in the homogeneous transitions considered in [17], which will be discussed elsewhere.

Our calculation suggests that the contact state of a drop on textured surface strongly depends on hysteresis. Simplification of being either in the Cassie or Wenzel state is precise only when CAH is unrealistically small. Experimental confirmation of our indication is possible. We could note that the CAHs of the Cassie and Wenzel states are quite different: such CAHs for intermediate states may be a good indirect measure of various contact states (*e.g.*, we

expect that the CAH for the P^* state is between those of the Wenzel and Cassie states); we can confirm our scenario by measuring such CAHs of a drop (which is gently deposited first and then gets an energy) for various sizes of the energy input. A more qualitative confirmation would require direct observation of the contact state with changing an energy supply.

* * *

The authors are grateful to D. QUÉRÉ, M. REYSSAT and M. LEOCMACH for discussions. KO thanks F. BROCHARD-WYART and P.-G. DE GENNES for a discussion on the critical size of the Wenzel nucleus. This work is supported by research grants, SAKURA (JSPS) and KAKENHI (MEXT, Japan).

REFERENCES

- [1] NEINHUIS C. and BARTHLOTT W., *Ann. Bot.*, **79** (1997) 667.
- [2] ONDA T., SHIBUICHI S., SATOH N. and TSUJII K., *Langmuir*, **12** (1996) 2125.
- [3] HOZUMI A. and TAKAI O., *Thin Solid Films*, **303** (1997) 222; TESHIMA K., SUGIMURA H., INOUE Y., TAKAI O. and TAKANO A., *Langmuir*, **19** (2003) 10624.
- [4] SWAIN P. S. and LIPOWSKY R., *Langmuir*, **14** (1998) 6772; SEEMANN R., BRINKMANN M., KRAMER E. J., LANGE F. F. and LIPOWSKY R., *Proc. Natl. Acad. Sci. U.S.A.*, **102** (2005) 1848.
- [5] BICO J., MARZOLIN C. and QUÉRÉ D., *Europhys. Lett.*, **47** (1999) 220; LAFUMA A. and QUÉRÉ D., *Nature Mater.*, **2** (2003) 457; CALLIES M. and QUÉRÉ D., *Soft Matter*, **1** (2005) 55.
- [6] HERMINGHAUS S., *Europhys. Lett.*, **52** (2000) 165; OTTEN A. and HERMINGHAUS S., *Langmuir*, **20** (2004) 2405.
- [7] ÖNER D. and MCCARTHY T. J., *Langmuir*, **16** (2000) 7777.
- [8] MIWA M., NAKAJIMA A., FUJISHIMA A., HASHIMOTO K. and WATANABE T., *Langmuir*, **16** (2000) 5754; YOSHIMITSU Z., NAKAJIMA A., WATANABE T. and HASHIMOTO K., *Langmuir*, **18** (2002) 5818.
- [9] PATANKAR N. A., *Langmuir*, **19** (2003) 1249; **20** (2004) 7097; 8209; HE B., PATANKAR N. A. and LEE J., *Langmuir*, **19** (2003) 4999.
- [10] MARMUR A., *Langmuir*, **19** (2003) 8343; **20** (2004) 3517.
- [11] NARHE R. and BEYSENS D., *Phys. Rev. Lett.*, **93** (2004) 076103; *Europhys. Lett.*, **75** (2006) 98.
- [12] DUPUIS A. and YEOMANS J. M., *Langmuir*, **21** (2005) 2624; *Europhys. Lett.*, **75** (2006) 105; KUSUMAATMAJA H., LÉOPOLDÈS J., DUPUIS A. and YEOMANS J. M., *Europhys. Lett.*, **73** (2006) 740.
- [13] WU X., ZHENG L. and WU D., *Langmuir*, **21** (2005) 2665.
- [14] LÉOPOLDÈS J. and BUCKNALL D. G., *Europhys. Lett.*, **72** (2005) 597.
- [15] SINGH S., HOUSTON J., VAN SWOL F. and BRINKER C. J., *Nature*, **442** (2006) 526.
- [16] DAW R., *Nature*, **436** (2005) 471; JIN M. *et al.*, *Adv. Mater.*, **17** (2005) 1977; JOURNET C., MOULINET S., YBERT C., PURCELL S. T. and BOCQUET L., *Europhys. Lett.*, **71** (2005) 104.
- [17] DE GENNES P.-G., BROCHARD-WYART F. and QUÉRÉ D., *Gouttes, Bulles, Perles et Ondes* (Belin, Paris) 2002.
- [18] ISHINO C., OKUMURA K. and QUÉRÉ D., *Europhys. Lett.*, **68** (2004) 419.
- [19] BARTOLO D., BOUAMRIRENE F., VERNEUIL É., BUGUIN A., SILBERZAN P. and MOULINET S., *Europhys. Lett.*, **74** (2006) 299; REYSSAT M., PÉPIN A., MARTY F., CHEN Y. and QUÉRÉ D., *Europhys. Lett.*, **74** (2006) 306.